Inversion and attribute-assisted hydraulically induced microseismic fracture characterization in the North Texas Barnett Shale

Xavier E. Refunjol and Kurt J. Marfurt, University of Oklahoma
Joël H. Le Calvez, Schlumberger

Once considered only as source rocks and seals, shale formations are now also considered as tight-porosity and low-permeability unconventional gas reservoirs. The classification as a reservoir is mainly technology- and economics-driven. Major gas (and significant oil) production from these plays is facilitated by massive hydraulic fracturing treatments that increase permeability and help to reactivate natural fractures. Natural faulting and fracturing are critical factors controlling present-day stress distribution, which in turn influences hydraulically induced fracture system development. Stimulation ultimately enhances reservoir drainage, yielding economically viable hydrocarbon production (Rutledge and Phillips, 2003; Gale et al., 2007; Miskimins, 2009). To better understand the created

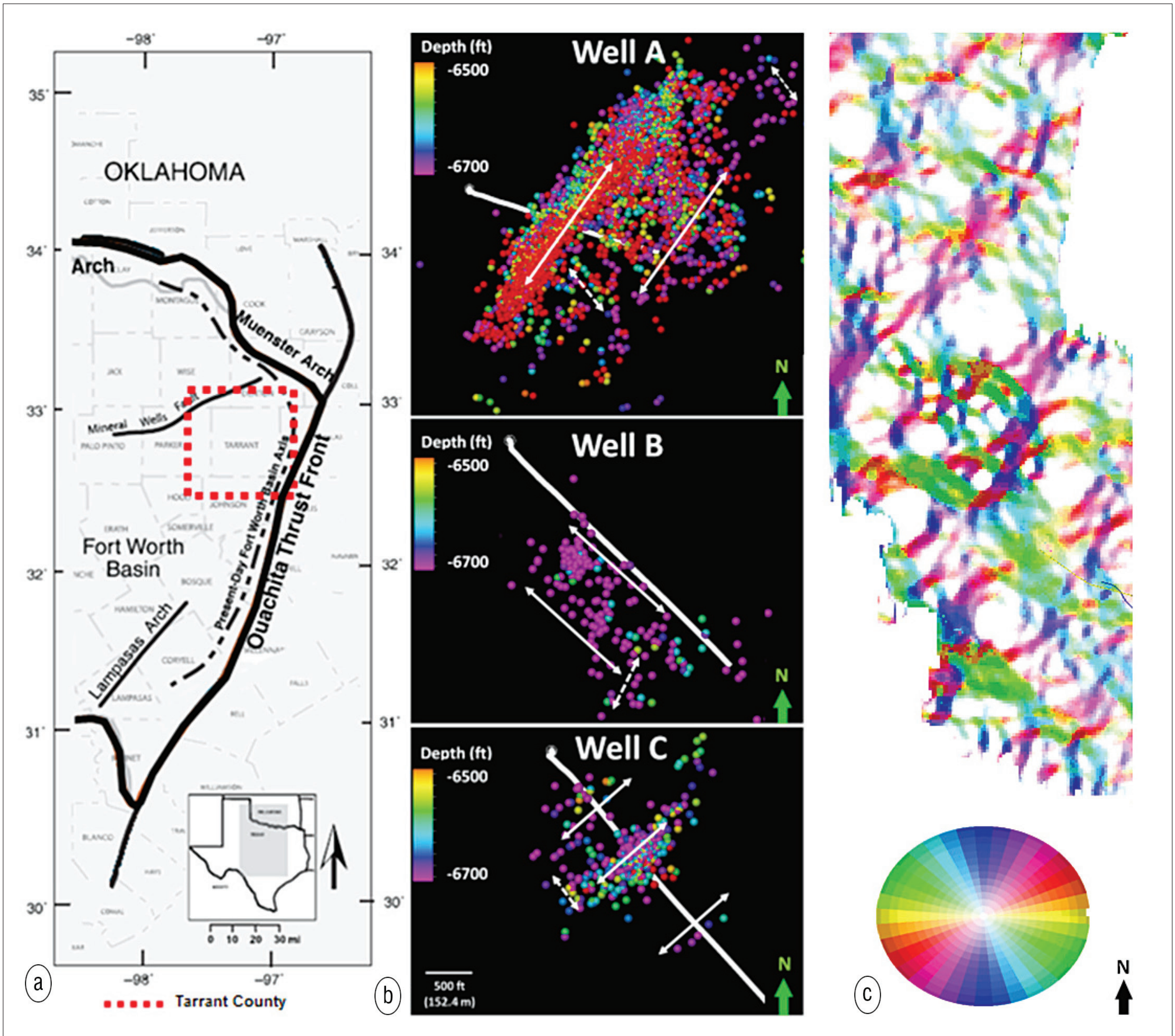

Figure 1. Mapped microseisms and surface seismic attributes within the Barnett Shale Formation show influence of regional structures. (a) Map of major structures surrounding the study area (Tarrant County) within the Bend Arch-Fort Worth Basin (modified from Pollastro et al., 2007). (b) Map views of hydraulically induced microseismic event locations (color-coded by depth) along horizontal Barnett Shale wells. Primary fracture trends (solid arrows) and secondary fracture trends (dashed arrows) mimic the major surrounding structures (i.e., Mineral Wells fault, Muenster Arch, Ouachita thrust front). (c) Time slice through the Barnett Shale Formation of most-positive principal curvature (k_1) strike modulated by the intensity of k_1 curvature. Strong NE-SW (magenta) and NW-SE (cyan) lineaments follow major surrounding structures

fracture geometry, borehole-based induced microseismicity monitoring may be used (Figure 1).

Thousands of borehole-based microseismic monitoring jobs have shown that expectations as to the hydraulically induced fracture system development are not always matched by observations. Knowing the current direction of maximum horizontal stress alone does not predict where fractures will develop (Rich and Ammerman, 2010). Further, because hydraulic fracture propagation is a time-dependent path-of-least-resistance process, other unaccounted-for factors can influence rock failure, such as the variability of the local stress field, formation anisotropy, and heterogeneous mineralogical composition. These factors can often result in variable fracture gradients and fracture zones (Jarvie et al., 2007). The variability also increases the risk of fracturing undesirable zones such as water-bearing formations.

To characterize the variations of rock properties within such formations, we generated seismic inversion volumes from a 14-m^2 prestack unmigrated seismic survey targeting the Barnett Shale within the Fort Worth Basin (Figure 1) using P- and S-impedance and Lamé parameters from density, shear, and compressional-velocity logs acquired in horizontal wells (Figure 2). Using microseismic data recorded before and after the corresponding seismic acquisition presents both the unaltered environment and the resulting fractured setting. We find that the locations of microseismic events correlate to specific values of the inverted surface seismic properties. While volumetric curvature volumes characterize fracture-prone flexures, amplitude inversions products such as acoustic and shear impedance characterize the matrix properties of the Barnett Shale most likely to fail. Further, Lamé parameters shed light on the extent of the fracture system into gas-bearing zones.

Together, surface seismic data and hydraulic fracture monitoring may be used to predict fracture system propagation. Such prediction can have a significant impact on reservoir stimulation planning, risk assessment, and economic evaluation. Accurate prediction and carefully targeted stimulation programs may lead to increased recovery rates through knowledge of possible drainage pathways from target zones.

Hydraulic stimulation and microseismicity in the Barnett Shale Formation

Acquisition and subsequent processing of the seismic signature of the Barnett Shale Formation's failure during hydraulic stimulation leads to maps of induced microseisms in 4D. Hydraulically induced fracture networks mapped in various formations around the world using borehole-based microseismic monitoring techniques correlate closely to stress states at various scales. Mapped fracture systems generally tend to propagate perpendicularly or nearly perpendicularly to the minimum horizontal stress, mimicking nearby structures like the Mineral Wells fault, Muenster Arch, and the Ouachita thrust front. Geological structures of the Bend Arch-Fort Worth Basin (Figure 1a) influence the induced hydraulic fracture system (Figure 1b) and can be imaged by volumetric curvature attributes derived from 3D surface seismic data (Figure 1c). Knowing the influence of local and regional stress regimes and structural features is a robust first step in characterizing the Barnett Shale's induced fracture systems.

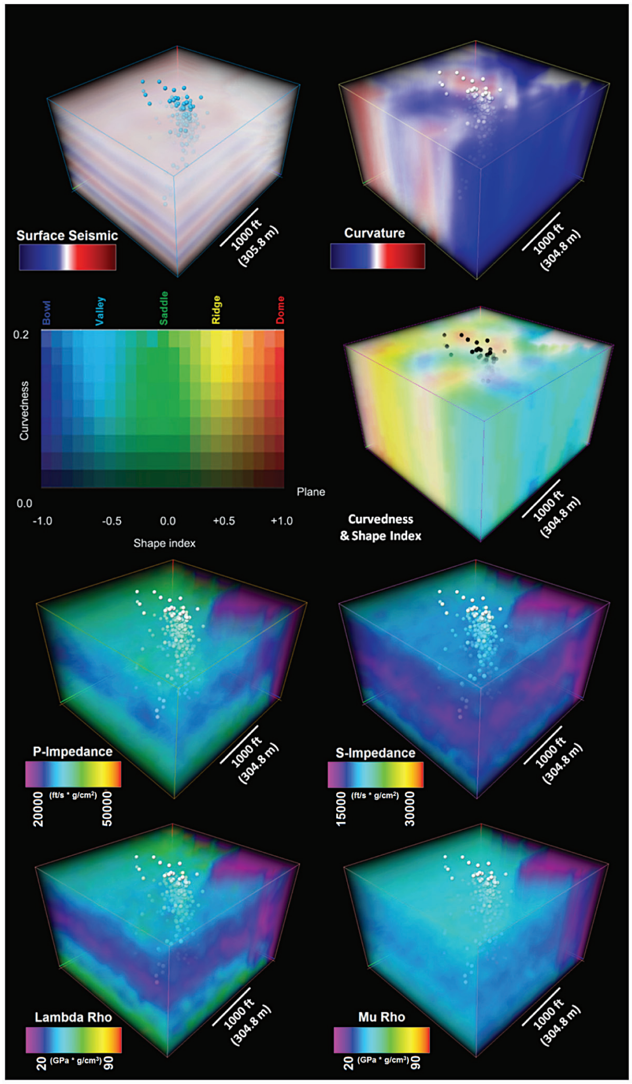

Figure 2. *Perspective view of mapped microseismic event loci within semitransparent attribute and inversion volumes. The cropped image above corresponds to the histogram analysis windows displayed in Figures 5 and 6. Microseismic events are associated with two stages of one of the lateral wells stimulated and analyzed in this study. The volumes were generated and cropped around the vicinity of the hydraulically induced microseisms. Curvature volumes were generated using the poststack seismic amplitude volume, while the inverted impedance and lambda rho, and mu rho volumes were generated from prestack amplitude gathers. Extracting the values of the properties at the location of each seemingly spatially unrelated event reveals that they occur in narrow ranges of each corresponding property. The strong correlation of values that characterize the fractured rock is in all stimulated wells studied within the Barnett Shale Formation analyzed in this project.*

Volumetric curvature attribute

Volumetric curvature attributes have successfully imaged a wide array of features that map regional tectonic features

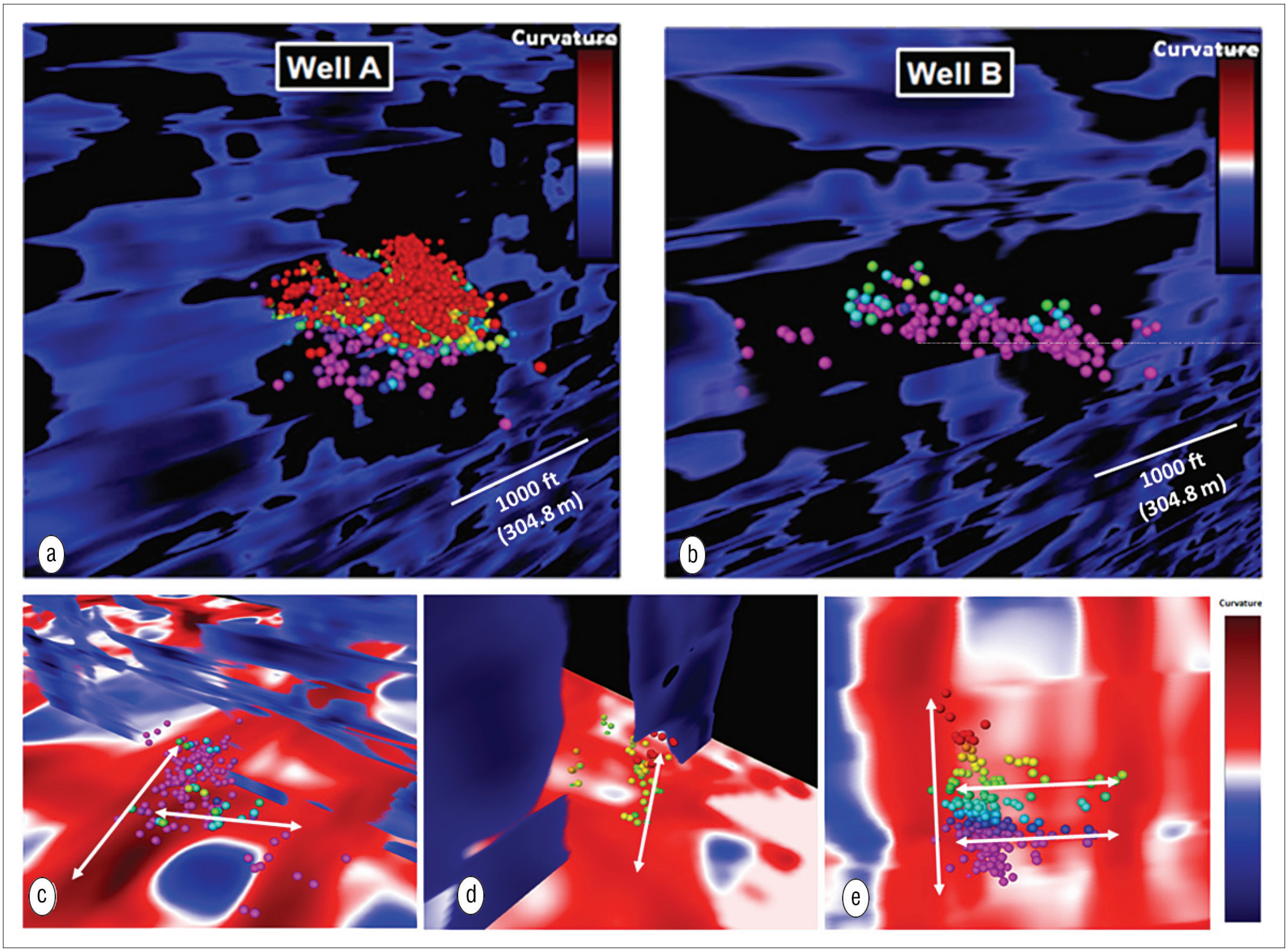

Figure 3. *Spatially, mapped microseisms induced in the Barnett Shale Formation tend to occur away from the most-negative (k_2) principal curvature and towards the most-positive principal curvature (k_1). (a) and (b) Vertical cross sections of long-wavelength k_2 through Barnett Shale microseismic clouds (color-coded in depth) induced by wells A and B, respectively. (c) and (d) Vertical cross sections of long-wavelength k_2 with time slices of k_1 through Barnett Shale microseismic event clouds. (e) Map view of microseisms on long-wavelength k_1 time slice.*

that correlate to zones of weakness and in turn influence the current stress regime. By using long-wavelength curvature as well as short-wavelength curvature, we can observe the different aspects of the same geology. As discussed in Chopra and Marfurt (2007), short-wavelength curvature delineates details within intense, highly localized fracture systems. Conversely, long-wavelength curvature often enhances subtle flexures correlative to fracture zones below seismic resolution and collapse features that result in broader depressions. In this study, long-wavelength most-positive and most-negative principal curvature show features that mimic the Mineral Wells and Ouachita thrust faults. Short-wavelength curvature, while also displaying a strong influence of the regional features, shows smaller secondary features at different azimuths (Figure 1c).

It has been established that hydraulically induced microseisms tend to occur within preexisting faults and fractures (Rothert and Shapiro, 2003; Iannacchione et al., 2004). Studies have shown favorable connections between curvature attribute and fractures (Masaferro et al., 2003; Lisle, 1994; Al-Dossary and Marfurt, 2006; Blumentritt et al., 2006). Applying curvature attributes to the area of study can serve as a tool to analyze the relationship between where microseisms occur and the corresponding surface seismic-derived formation properties that could cause them, like flexure shape and curvature signs. Figure 3 shows how microseisms occur away from the most-negative principal curvature (blue) and toward the most positive principal curvature (red), as discussed in Refunjol et al. (2010a).

To relate the curvature attribute with the structural characteristics of the subsurface, 3D quadratic shapes can be described using values of k_1 and k_2. The fractures correlate to anticlinal 3D shapes like domes, ridges, and saddles (Figure 4).

Acoustic impedance inversion

Similar to the structural relationship between induced fractures and volumetric curvature, we hypothesize that properties like density, acoustic impedance, and V_P/V_S can also be correlated to where hydraulically induced microseismic fractures occur.

We were interested in understanding the factors that

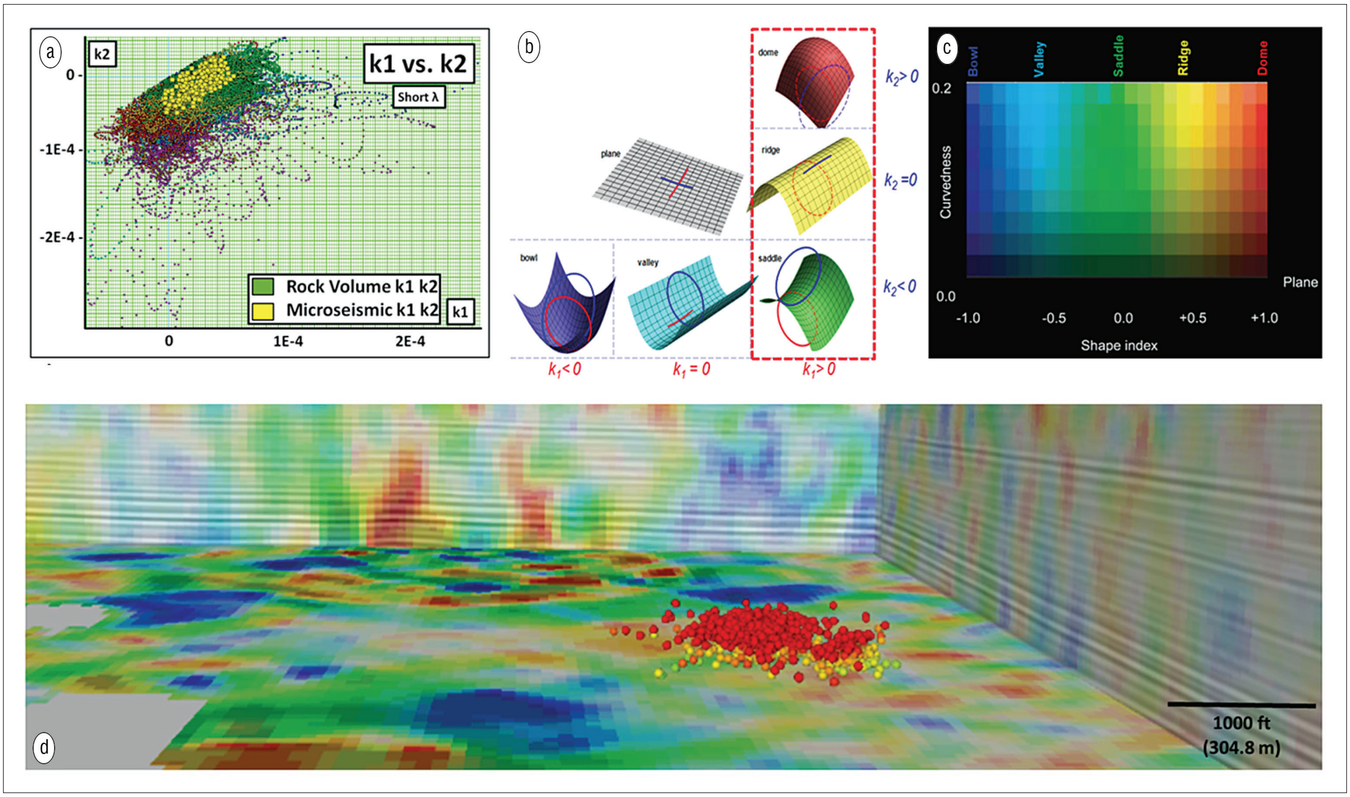

Figure 4. *Curvature, shape index, and curvedness attributes help characterize the behavior of the Barnett Shale rock surrounding induced fractures. (a) Short-wavelength* k_1 *versus* k_2 *crossplots of microseismic event values and the values of the rock volume that surrounds them. Mapped events strongly correlate to dome, ridge, and saddle shapes of 4b. (b) Six basic 3D quadratic shapes described by most-positive (*k_1*) and most-negative (*k_2*) curvature values (modified from Mai, 2010). (c) 2D color table displaying the shale index (hue) modulated by curvedness (lightness). Highly curved features are plotted as pure color, while planar features are displayed in black (modified from Guo et al., 2008). (d) Shape index modulated by curvedness corendered with seismic amplitude on vertical slice for general behavior of 3D shapes surrounding a stimulated well. Shape index modulated by curvedness on time slice along the Barnett Shale Formation. Mapped microseisms correlate to dome, ridge and saddle structural components (red-yellow-green).*

led to the subsequent known failure loci, and the relationship between mapped microseisms and the composition of the volumes where they occur (Figure 2). To achieve this we generated seismic P-impedance and S-impedance inversion volumes (Figure 5) using a commercial model-based inversion algorithm. The background model was generated using P- and S-wave sonic logs as well as density logs acquired before the hydraulic fracture process. The resulting correlation suggests that 3D surface-seismic-derived inversion volumes may serve as a tool to help design hydraulic stimulation programs using a priori knowledge of the most likely fracture propagation trends and failure loci.

By design, the microseisms occur primarily within the stimulated formation, in this case the lower Barnett Shale Formation. Assuming data have been properly processed using an accurate and representative velocity model, and that resulting hypocentral loci have small associated uncertainty ellipsoids, locations of the microseismic events in the Barnett Shale Formation have a good correlation to the inversion volumes, where they correspond to a narrow range of values for each property in all stimulation stages of the studied wells, regardless of their orientation and location.

P-impedance and S-impedance histograms of the values corresponding to the microseisms against impedance values from the volume surrounding the stimulated area (Figure 2) suggest that hydraulically stimulated rocks preferably fail within low-impedance zones (Figure 5). Furthermore, in wells where stimulation extended beyond the target formation, we find that fractures occur in the lower end of the impedance spectrum corresponding to each formation, as discussed in Refunjol et al. (2010b).

In order to further investigate this relationship, we generated P-impedance versus S-impedance plots of the stimulated rock about the wells and those at the microseism locations. Figure 5 (bottom) shows that there is greater occurrence of events for low values of Z_P and Z_S. Furthermore, events show a distinct linear trend corresponding to a value of Z_P/Z_S = 1.65 or a Poisson's ratio of ~0.27. This crossplot suggests that we can use the inversion of surface seismic data to predict subsurface zones where the rock is more likely to fail and might serve as reservoir drainage pathways.

Similar to the impedance results, density histograms show preferential fracturing toward the lower end of the density spectrum. In other words, the observed events occur in the less dense areas of the rock volume. It is possible that events occurring in even lower-density rock might have aseismic behavior, or generate low nonrecordable energy.

Although the values of Poisson's ratio are low, Young's

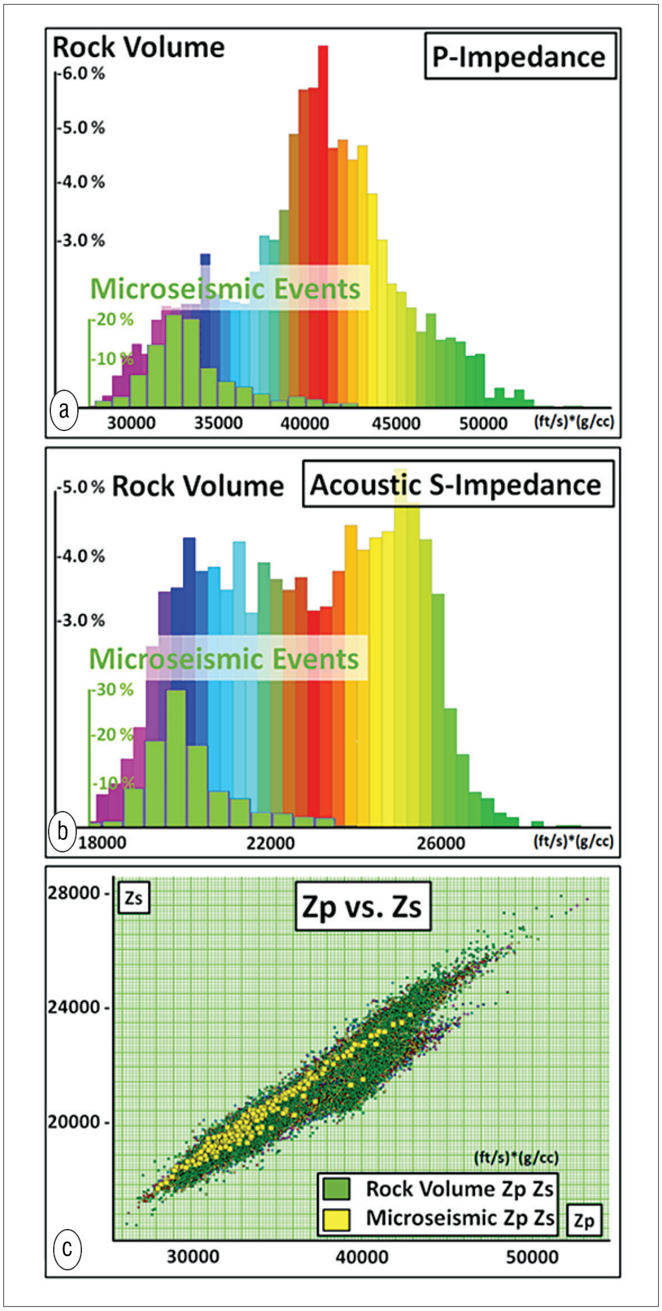

Figure 5. *For a more quantitative approach, we plotted histograms of the impedance values corresponding to the microseisms with the (a) P-impedance and (b) S-impedance values found in the volume surrounding the stimulated Barnett Shale. Events fall within very similar values of the inverted impedances, where the rock appears more prone to fracturing throughout all stages and wells within our study area. The fractured zones fall in the lower end of the impedance spectrum of each fractured formation, with a linear trend in the Zp versus Zs crossplot (c).*

modulus is also low, which contradicts the general assumption that hydraulic stimulation preferentially fractures brittle rock as it generates larger fracture systems and ultimately a more efficient drainage pathway (Grieser et al., 2007; Rickman et al., 2008). Because all stages of all four fractured wells present the same behavior, we hypothesize that low-impedance zones in our survey are more likely to fracture given that hydraulic fracture propagation is a time-dependent path-of-least-resistance process. This observation is in agreement with those of Rutledge and Phillips (2003), who find shear activation of fractures to be correlated to low impedance. Further, at subseismic scale, Gale et al. (2007) have found that calcite-cemented healed fractures like the ones observed in the Barnett Shale Formation are more easily propped open than undisturbed shale. Their investigation shows that the tensile strength of the contact between the calcite fracture fill and the shale wall rock is low, leading to weak fracture-host boundary and a path of least resistance for hydraulic fracture propagation.

Lamé parameters

Having established the structural and compositional characteristics of fracture-prone Barnett rock, the next phase was to evaluate if the desired zones were being stimulated. We derived Lamé parameters λ and μ, incompressibility and rigidity respectively, from the acoustic impedances (Chopra and Pruden, 2003). These parameters have been used to improve delineation of reservoirs because incompressibility is more sensitive to the pore fluids than to the matrix, whereas the rigidity is influenced by the matrix connectivity only (Dufour et al., 2002). In Figure 6 we examine the relationship between Lamé parameters of microseism event locations to the lambda-rho and mu-rho values of the surrounding rock.

Microseisms associated with the well depicted in Figure 6 show two modes. The first mode has a strong correlation to low incompressibility and rigidity values that correspond to those of the Barnett Shale. In these cases, the lowest $\lambda\rho$ versus $\mu\rho$ zones of the Barnett Shale mode are fracture-prone. The second mode indicates the high values of the Ordovician carbonates mode are the ones fractured.

In Figure 6 (bottom), we display a crossplot of $\lambda\rho$ versus $\mu\rho$ in the surrounding rock (in green) and values at the microseism event locations (in yellow). We note a linear trend of the microseismic points, fracturing the Barnett Shale and not the Ordovician carbonates.

Limitations

Because wells logged before stimulation represent the unfractured medium, and seismic acquired after stimulation images the fractured medium, certain theoretical modeling errors could be expected in the vicinity of the stimulation wells. It is possible that extensive fracturing could change the medium and lower its density and impedance values from its unfractured state. However, similarities between pre- and post-stimulation seismic imply that any possible change is below the seismic resolution and that both instances can be effectively used for microseismic characterization. Further, the stimulations in this study are limited to only two stages in certain wells, resulting in a modest alteration of the matrix formation. These types of changes might be observable with a high-density and oversampled surface seismic survey or with core sample testing. Processing of the raw microseismic data, rather than using processed data (i.e., hypocentral locations only) would provide information on background

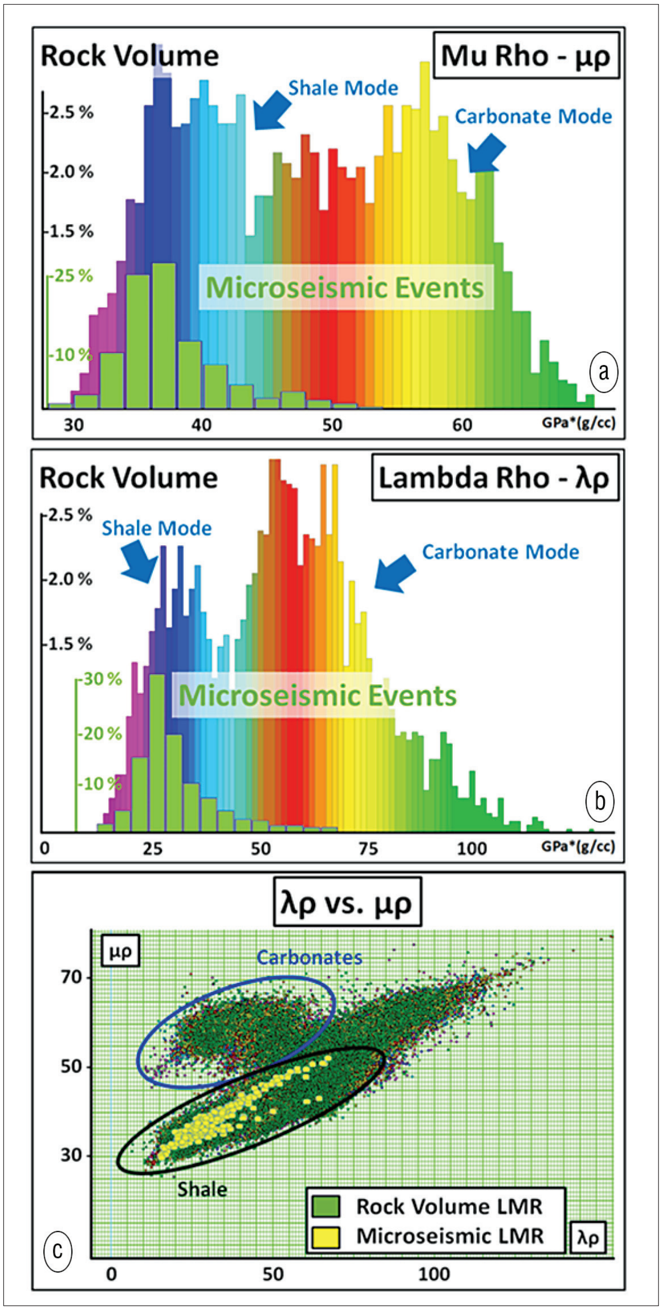

__Figure 6.__ Derived Lamé parameters μ (rigidity) and λ (incompressibility) expressed as (a) μρ and (b) λρ histograms. These parameters have been used to improve delineation of reservoirs, given that incompressibility is more sensitive to the pore fluids than to the matrix; whereas the rigidity is influenced by the matrix connectivity only (Dufour et al., 2002). If the values of hydrocarbon-rich zones are known, this serves to validate the effectiveness of such zones' stimulation. (c) Illustration of the predominance of fractures within shale rock.

noise and its impact on time picks and associated hodogram analysis (uncertainty) as well as source parameters and potentially focal mechanisms. Similarly, the accuracy of our inversion volumes could be increased significantly with the use of a fully processed prestack migrated seismic data set. This would generate more precise P- and S-impedance, V_P/V_S, and Lamé parameters volumes and the microseism values associated with them.

Conclusions

We propose characterizing fracture-prone zones in the subsurface from prestack P- and S-impedance inversion of Barnett Shale surface seismic data calibrated to microseismic event locations. Coupling this observation with the correlation of induced fractures with curvature anomalies, we anticipate a workflow that provides a priori knowledge of potential fracture system distribution. Careful characterization of the structural and compositional properties of the fractured zones corresponding to recorded microseisms offers a predictive framework for fracture-prone zones within the Barnett Shale formation. Such prediction can lead to increased recovery rates from a hydraulic stimulation in other unconventional plays. TLE

Appendix

Curvature. The curvature of a surface at a particular point is the inverse of a circle's radius which is tangent to that surface at that point and, by convention, positive curvature is concave downward, and negative curvature is concave upward (Roberts, 2001; Blumentritt et al., 2006).

Curvedness. This is a measure of the total deformation of a horizon given by $c = 1/2(k_{min}{}^2 + k_{max}{}^2)^{1/2}$, where k_{min} and k_{max} are the minimum and maximum curvatures (Roberts, 2001; Chopra and Marfurt 2007a).

Principal curvatures. The principal curvatures are the most-positive (k_1) and most-negative (k_2) signed curvatures of a quadratic surface that have dip; k_1 and k_2 are always perpendicular to each other (Roberts, 2001; Chopra and Marfurt 2007a).

References

Al-Dossary, S., and K. J. Marfurt, 2006, 3D volumetric multispectral estimates of reflector curvature and rotation: Geophysics, **71**, no. 5, 41–51, doi:10.1190/1.2242449.

Blumentritt, C. H., K. J. Marfurt, and E. C. Sullivan, 2006, Volume-based curvature computations illuminate fracture orientations—Early to mid-Paleozoic, Central Basin Platform, west Texas: Geophysics, **71**, no. 5, B159–B166, doi:10.1190/1.2335581.

Chopra, S. and K. J. Marfurt, 2007a, Seismic attributes for prospect identification and reservoir characterization: SEG.

Chopra, S. and K. J. Marfurt, 2007b, Volumetric curvature attributes add value to 3D seismic data interpretation: The Leading Edge, **26**, no. 7, 856–867, doi:10.1190/1.2756864.

Chopra, S. and D. Pruden, 2003, Multiattribute seismic analysis on AVO-derived parameters—A case study: The Leading Edge, **22**, no. 10, 998–1002, doi:10.1190/1.1623640.

Dufour, J., J. Squires, W. N. Goodway, A. Edmunds, and I. Shook, 2002, Integrated geological and geophysical interpretation case study, and Lamé rock parameter extractions using AVO analysis on the Blackfoot 3C–3D seismic data, southern Alberta, Canada: Geophysics, **67**, no. 1, 27–37, doi:10.1190/1.1451319.

Gale, J. F., R. M. Reed, and J. Holder, 2007, Natural fractures in the Barnett Shale and their importance for hydraulic fracture treatments: AAPG Bulletin, **91**, no. 4, 603–622, doi:10.1306/11010606061.

Grieser, B. and J. Bray, 2007, Identification of production potential in unconventional reservoirs: SPE paper 106623.

Guo, H., S. Lewis, and K. J. Marfurt, 2008, Mapping multiple attributes to three- and four-component color models—A tutorial:

Geophysics, **73**, no. 3, 7–19, doi:10.1190/1.2903819.
Iannacchione, A. T., T. Batchler, and T. E. Marshall, 2004, Mapping hazards with microseismic technology to anticipate roof falls—A case study: 23rd International Conference on Ground Control in Mining, 327–333.
Jarvie, D. M., R. J. Hill, T. E. Ruble, and R. M. Pollastro, 2007, Unconventional shale-gas systems: The Mississippian Barnett Shale of north-central Texas as one model for thermogenic shale-gas assessment: AAPG Bulletin, **91**, no. 4, 475–499, doi:10.1306/12190606068.
Lisle, R. J., 1994, Detection of zones of abnormal strains in structures using Gaussian curvature analysis: AAPG Bulletin, 78, 1811–1819.
Mai, H. T., 2010, Seismic attribute analysis and its application to mapping folds and fractures: Ph.D. dissertation, University of Oklahoma.
Masaferro, J. L., M. Bulnes, J. Poblet, and M. Casson, 2003, Kinematic evolution and fracture prediction of the Valle Morado structure inferred from 3-D seismic data, Salta Province, northwest Argentina: AAPG Bulletin, **87**, no. 7, 1083–1104, doi:10.1306/02070301102.
Miskimins, J., 2009, The importance of geophysical and petrophysical data integration for the hydraulic fracturing of unconventional reservoirs: The Leading Edge, **28**, no. 7, 844–849, doi:10.1190/1.3167787.
Pollastro, R. M., D. M. Jarvie, R. J. Hill, and C. W. Adams, 2007, Geologic framework of the Mississippian Barnett Shale, Barnet-Paleozoic total petroleum system, Bend arch-Fort Worth Basin, Texas: AAPG Bulletin, **91**, no. 4, 405–436, doi:10.1306/10300606008.
Refunjol, X. E., K. M. Keranen, and K. J. Marfurt, 2010a, Inversion and attribute-assisted hydraulically induced microseismic fracture prediction: A North Texas Barnett Shale case study: 80th Annual International Meeting, SEG, Expanded Abstracts, 2161–2165.
Refunjol, X. E., J. H. Le Calvez, K. J. Marfurt, and K. M. Keranen, 2010b, Predicting hydraulically induced microseismic fractures from seismic inversion volumes: A North Texas Barnett Shale case study: Microseismicity: Beyond Dots in a Box Workshop, 80th Annual International Meeting, SEG.
Rich, J. P. and M. Ammerman, 2010, Unconventional geophysics for unconventional plays: SPE paper 131779.
Rickman, R., M. Mullen, E. Petre, B. Grieser, and D. Kundert, 2008, A practical use of shale petrophysics for stimulation design optimization: SPE paper 115258.
Roberts, A., 2001, Curvature attributes and their application to 3D interpreted horizons: First Break, **19**, no. 2, 85–100, doi:10.1046/j.0263–5046.2001.00142.x.
Rothert, E. and S. A. Shapiro, 2003, Microseismic monitoring of borehole fluid injections: Data modeling and inversion for hydraulic properties of rocks: Geophysics, **68**, no. 2, 685–689, doi:10.1190/1.1567239.
Rutledge, J. T. and W. S. Phillips, 2003, Hydraulic stimulation of natural fractures as revealed by induced microearthquakes, Carthage Cotton Valley gas field, east Texas: Geophysics, **68**, no. 2, 441–452, doi:10.1190/1.1567212.

Acknowledgments: The authors thank Devon Energy for providing data, financial support for this investigation, and permission to publish this work. We thank Katie M. Keranen at the University of Oklahoma for her important contributions during this investigation. Xavier Refunjol is now with Swift Energy.

Corresponding author: xavier.refunjol@swiftenergy.com